Time-Resolved Observation of Discrete and Continuous Magnetohydrodynamic Dynamo in the Reversed-Field Pinch Edge

H. Ji, A. F. Almagri, S. C. Prager, and J. S. Sarff
Department of Physics, University of Wisconsin, Madison, Wisconsin 53706
(Received 7 January 1994)

We report the first experimental verification of the magnetohydrodynamic (MHD) dynamo in the reversed-field pinch (RFP). A burst of MHD dynamo electric field is observed during the sawtooth crash, followed by an increase in the local parallel current in the Madison Symmetric Torus RFP edge. By measuring each term, the parallel MHD mean-field Ohm's law is observed to hold within experimental error bars both between and during sawtooth crashes.

PACS numbers: 52.55.Hc, 52.25.Gj, 52.35.Ra

The dynamo phenomenon, in which the magnetic-field-aligned electric current is self-generated by plasma dynamics, has been a mystery in magnetically confined laboratory plasmas and astrophysical plasmas for many decades. The reversed-field-pinch (RFP) toroidal plasma, in which the toroidal field reverses its direction at the edge, is a particularly vivid example of the dynamo effect. In the RFP, the externally applied electric field is in the toroidal direction. Thus, the poloidal current near the edge, essentially parallel to the magnetic field, is generated and maintained by the dynamo. In the widely studied magnetohydrodynamic (MHD) dynamo model, a fluctuation-induced electromotive electric field $\langle \tilde{\boldsymbol{v}} \times \tilde{\boldsymbol{B}} \rangle_{\|}$ sustains the field-aligned current against resistive decay in the parallel Ohm's law [1]

$$E_{\|} + \langle \tilde{\boldsymbol{v}} \times \tilde{\boldsymbol{B}} \rangle_{\|} = \eta j_{\|} ,$$

where $E_{\|}$ is the equilibrium electric field parallel to the magnetic field, η the electric resistivity, $j_{\|}$ the parallel equilibrium current, $\tilde{\boldsymbol{v}}$ and $\tilde{\boldsymbol{B}}$ are the fluctuating fluid velocity and magnetic field, respectively, and $\langle \cdots \rangle$ denotes an average over an equilibrium flux surface. On the other hand, the kinetic dynamo theory (KDT) [2,3] assumes that the dynamo is driven by radial diffusion of the parallel current due to a prescribed stochastic magnetic field. The KDT model is supported [4] by the existence of a small population of fast electrons detected at the edge with a temperature comparable to core electrons. These fast electrons carry most of the edge parallel current [5,6], but the current diffusion hypothesized for their existence has never been directly measured.

The MHD model has been intensively investigated by a large number of authors through nonlinear computation [7], and it agrees fairly well with experimental tearing mode spectra and their nonlinear mode interactions. However, measurements in the REPUTE-1 RFP edge have shown [8] that the MHD dynamo electric field is not sufficient to account for $\eta j_{\|} - E_{\|}$. Contrariwise, recent measurements in a spheromak [9] indicate nonzero MHD dynamo electric fields.

In this Letter, we report a first experimental verification of the MHD dynamo in the RFP edge. In the Madison Symmetric Torus (MST) RFP an additional test of the dynamo is allowed by the presence of clear sawtooth oscillations [10]. The sawtooth crash is a discrete dynamo event during which substantial toroidal flux (and edge poloidal current) is generated. We observe the MHD dynamo electric field both as a burst during the sawtooth crash and continuously between the crashes, sufficient to sustain the parallel current. The difference in dynamo mechanisms active in MST and REPUTE is likely due to the substantially different edge conditions, as discussed later.

In MST and the earlier experiments the MHD dynamo term is inferred from probe measurement of the fluctuating electric field ($\tilde{\boldsymbol{v}}$ is not measured directly). To interpret the measured quantities, we consider the generalized Ohm's law [11],

$$-\frac{m_e}{e^2 n}\frac{\partial \boldsymbol{j}}{\partial t} + \boldsymbol{E} + \boldsymbol{v} \times \boldsymbol{B} - \frac{1}{en}\boldsymbol{j} \times \boldsymbol{B} + \frac{\nabla P_e}{en} = \eta \boldsymbol{j} , \tag{1}$$

where n is the electron density and P_e the electron pressure. By splitting every quantity into mean (denoted by subscript 0) and fluctuating (denoted by tildes) parts, averaging over a flux surface, and taking the parallel component, the parallel Ohm's law in a turbulent plasma becomes

$$\eta_{\|} j_{\|0} - E_{\|0} = \langle \tilde{\boldsymbol{v}} \times \tilde{\boldsymbol{B}} \rangle_{\|} - \langle \tilde{\boldsymbol{j}} \times \tilde{\boldsymbol{B}} \rangle_{\|}/en , \tag{2}$$

where we have neglected two small $\partial j_{\|}/\partial t$ and $\langle \tilde{\eta} \tilde{j}_{\|} \rangle$ terms, as appropriate for the experimental condition. The right-hand side includes the usual $\langle \tilde{\boldsymbol{v}} \times \tilde{\boldsymbol{B}} \rangle$ term and the Hall term previously measured to be small in MST [12].

An alternative form of the parallel Ohm's law can be derived by substituting the perpendicular component of Eq. (1), $\tilde{\boldsymbol{v}}_{\perp} - \tilde{\boldsymbol{j}}_{\perp}/en \approx (\tilde{\boldsymbol{E}}_{\perp} \times \boldsymbol{B}_0 + \nabla_{\perp}\tilde{P}_e \times \boldsymbol{B}_0/en)/B^2$, into Eq. (2) to yield

$$\eta_{\|} j_{\|0} - E_{\|0} = \langle \tilde{\boldsymbol{E}}_{\perp} \cdot \tilde{\boldsymbol{b}}_{\perp} \rangle + \langle \nabla_{\perp}\tilde{P}_e \cdot \tilde{\boldsymbol{b}}_{\perp} \rangle s/en , \tag{3}$$

where $\boldsymbol{b} \equiv \boldsymbol{B}/B$. For simplicity of presentation, we have ignored the density fluctuations $\tilde{n}$, which would add a term $\langle \tilde{n} \nabla_{\|} \tilde{P}_e \rangle/en^2$ in both Eqs. (2) and (3), but would not change our conclusions.

0031-9007/94/73(5)/668(4)$06.00
© 1994 The American Physical Society

Interestingly, note that the usual $\langle \tilde{\boldsymbol{v}} \times \tilde{\boldsymbol{B}} \rangle$ term consists of both $\langle \tilde{\boldsymbol{E}}_\perp \cdot \tilde{\boldsymbol{b}}_\perp \rangle$ and $\langle \nabla_\perp \tilde{P}_e \cdot \tilde{\boldsymbol{b}}_\perp \rangle / en$ terms, by comparing Eqs. (2) and (3). The first term represents the contribution to $\tilde{\boldsymbol{v}}$ from the fluctuating $\boldsymbol{E} \times \boldsymbol{B}$ drift, while the second term is the contribution from the fluctuating diamagnetic drift. The latter one, which is $\propto \partial \langle \tilde{P}_e \tilde{b}_r \rangle / \partial r$ in the shearless limit, represents current diffusion in *space* due to $\tilde{b}_r$ and includes the KDT mechanism. However, this term is not included in the pressureless MHD computations [7]. Therefore, we identify the first term $\langle \tilde{\boldsymbol{E}}_\perp \cdot \tilde{\boldsymbol{b}}_\perp \rangle$ as "the MHD dynamo term," usually referred to as $\langle \tilde{\boldsymbol{v}} \times \tilde{\boldsymbol{B}} \rangle$. The experiments described here are aimed to measure $\langle \tilde{\boldsymbol{E}}_\perp \cdot \tilde{\boldsymbol{b}}_\perp \rangle$ which has two large components, $\langle \tilde{E}_t \tilde{b}_t \rangle$ and $\langle \tilde{E}_r \tilde{b}_r \rangle$, since $B_p \gg B_t$ in RFP edge.

The MST [13] is a large RFP device with major radius R of 1.50 m, minor radius a of 0.52 m, and plasma current up to 700 kA. The experiments reported here were carried out at the relatively low plasma current of $\simeq$210 kA to avoid heat damage to the inserted probe and at sufficient density (chord-averaged density $\bar{n_e} \simeq 1.0 \times 10^{19}/\mathrm{m}^3$) to minimize disturbance of the triple probe measurement by the fast electrons. Density scan experiments have shown that the influence of the fast electrons on probe measurement is significant only at low density ($\bar{n_e} < 0.8 \times 10^{19}/\mathrm{m}^3$). All measurements presented here are taken during $t = 13$–25 ms around the current flattop.

Two versions of a complex probe [14] have been constructed to measure $\langle \tilde{E}_t \tilde{b}_t \rangle$ and $\langle \tilde{E}_r \tilde{b}_r \rangle$, respectively. Each version consists of two triple probes to measure electron temperature T_e, density n, and floating potential V_f at two locations separated by 1.27 cm toroidally or 0.25 cm radially. The electrostatic components of electric fields E_t and E_r can be obtained from the difference in plasma potential $V_p = V_f + cT_e$, where $c \simeq 2.5$ (0.8) for E_t (E_r) calculated from the electron-ion collection area ratio at the different orientation of the probe tips with respect to the magnetic field [14]. (The uncertainty in c does not change our conclusions.) Magnetic pickup coils for B_t and B_r are also installed to infer $\langle \tilde{E}_t \tilde{b}_t \rangle$ and $\langle \tilde{E}_r \tilde{b}_r \rangle$. A separate, small, insertable Rogowskii coil probe [15] measures the local poloidal (parallel) current.

The measurements at each radial position were carried out in 30 identical discharges with 150 sawtooth crashes. To obtain ensemble-averaged quantities (such as cross correlations) with time-resolved information during a sawtooth crash, an ensemble is constructed from time samples time referenced to a crash instead of the conventional cross-spectra method for stationary turbulence. Since the plasma rotates in the laboratory frame, this method is equivalent to flux surface averaging even though the measurement position is fixed. Using phase-shifted fluctuations calculated via the fast Fourier transform, we calculate the time-resolved coherence γ and phase shift θ between two fluctuating quantities.

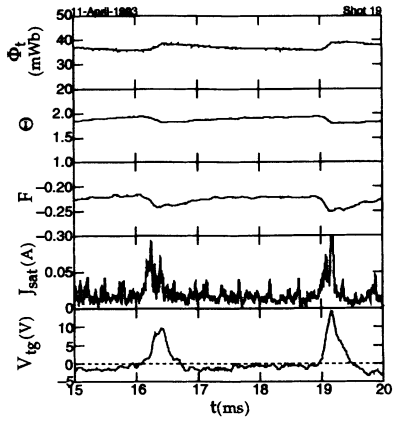

FIG. 1. Wave forms of toroidal flux Φ_t, pinch parameter Θ, reversal parameter F, ion saturation current J_{sat} measured by the triple probe at $r/a = 0.98$, and voltage across toroidal gap in the shell V_{tg} during two sawtooth oscillations.

Sawtooth oscillations in MST represent discrete dynamo events. Figure 1 illustrates field generation and relaxation over two sawtooth oscillations spanning 5 ms. Strong spontaneous field generation is evident in the sudden increase of the toroidal flux Φ_t during a sawtooth crash (in $\sim$0.1 ms). Between crashes, flux generation (opposing resistive decay) is present but mild. The decreases in the pinch parameter $\Theta \equiv B_p(a)/(\Phi_t/\pi a^2)$ and the reversal parameter $F \equiv B_t(a)/(\Phi_t/\pi a^2)$ show that the plasma relaxes toward the minimum energy state with a flatter current profile, i.e., current decreases at the core and increases at the edge. The edge density and electron temperature also increase during a crash, as represented in Fig. 1 by the ion saturation current J_{sat} measured by the triple probe at $r/a = 0.98$. The time derivative of the flux, measurable as the voltage across the toroidal gap in the shell, V_{tg}, is employed as a trigger for the sawtooth ensemble averaging and as a time reference throughout the paper.

Ensemble-averaged fluctuation amplitudes, coherence, and phase shift during one sawtooth, measured at 5 cm from the wall ($r/a = 0.90$), are shown in Fig. 2. Fluctuation amplitudes peak at the sawtooth crash (except for $|\tilde{E}_t|$), while the coherence is low ($\simeq 0.1$) and the phase shift is almost π(antiphase) between $\tilde{\boldsymbol{E}}_\perp$ and $\tilde{\boldsymbol{B}}_\perp$. ($\gamma_{E_t B_t}$ and $\theta_{E_t B_t}$ are not shown, but they are similar to their counterparts of $\langle \tilde{E}_r \tilde{b}_r \rangle$.)

The two components of $\langle \tilde{\boldsymbol{E}}_\perp \cdot \tilde{\boldsymbol{b}}_\perp \rangle$ measured at $r/a = 0.90$ are shown in Fig. 3. Both $\langle \tilde{E}_t \tilde{b}_t \rangle$ and $\langle \tilde{E}_r \tilde{b}_r \rangle$ peak during the crash. The local poloidal current density j_p keeps rising during the crash and peaks at the end of the crash, consistent with current profile flattening.

To establish the strength of the MHD dynamo term we compare it to other measured terms in Ohm's law [Eq. (3)]. In Fig. 4(a), we compare the measured MHD dynamo electric field to the resistive term $\eta j_\parallel$, where η

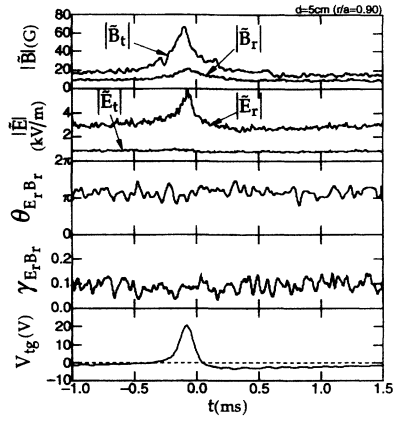

FIG. 2. Ensemble-averaged fluctuation amplitudes, coherence, and phase shift during one sawtooth cycle, measured at $r/a = 0.90$. The toroidal gap voltage, V_{tg}, marks the timing of the sawtooth crash.

is Spitzer's resistivity calculated from the measured local T_e but estimated $Z_{eff} = 3$. In spite of large experimental error bars, fairly good agreement can be seen between $\langle \tilde{E}_\perp \cdot \tilde{b}_\perp \rangle$ and $\eta j_\parallel$ except for the burst of dynamo electric field during the crash. The electric field term is included in Fig. 4(b) which compares $\langle \tilde{E}_\perp \cdot \tilde{b}_\perp \rangle$ to $\eta j_\parallel - E_\parallel$. The parallel electric field at the edge is given by

$$E_\parallel(r) \approx \left(V_{tg} - 2\pi \int_r^a \dot{B}_t r \, dr \right) / 2\pi r ,$$

where the first term dominates. By including the electric field, Fig. 4(b) shows good agreement between $\langle \tilde{E}_\perp \cdot \tilde{b}_\perp \rangle$ and $\eta j_\parallel - E_\parallel$ at all times within experimental uncertainty.

The emerging physical picture of MST edge dynamo can be separated into two stages: (a) a continuous dynamo electric field drives equilibrium poloidal current between the sawtooth crashes and (b) the crash generates a burst of (discrete) dynamo electric field which is largely balanced by an inductive $E_\parallel$ during the $j_\parallel$ rising phase. The effective inductance can be estimated as $l = E_\parallel / (dj_\parallel/dt) \sim 6 \times 10^{-9}$ H m. The resulting L/R time constant is $\tau = l/\eta \sim 0.2$ ms, consistent with the decay time of $j_\parallel$ after the sawteeth.

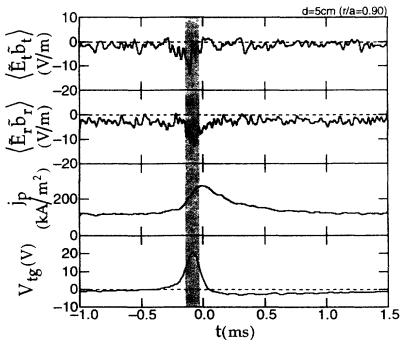

FIG. 3. Ensemble-averaged MHD dynamo electric fields and local parallel current density during one sawtooth crash, measured at $r/a = 0.90$.

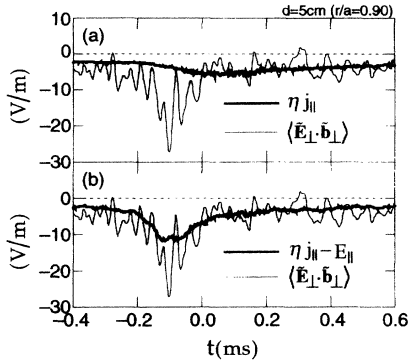

FIG. 4. Comparison of MHD dynamo electric field $\langle \tilde{E}_\perp \cdot \tilde{b}_\perp \rangle$ to (a) $\eta j_\parallel$ and (b) $\eta j_\parallel - E_\parallel$ during one sawtooth crash. Rapid oscillations in $\langle \tilde{E}_\perp \cdot \tilde{b}_\perp \rangle$ indicate experimental uncertainty.

The radial profiles of $\langle \tilde{E}_\perp \cdot \tilde{b}_\perp \rangle$ and $\eta j_\parallel - E_\parallel$ are shown in Fig. 5. The parallel MHD Ohm's law [Eq. (3) without the second term in the right-hand side] holds both between and during the sawtooth events within the experimental error bars. This result provides experimental verification of MHD dynamo hypothesis in the RFP.

The MST result is in contrast with the first such measurement [8] performed in the REPUTE-1 RFP edge, in which the MHD dynamo electric field is not sufficient to account for $\eta j_\parallel - E_\parallel$. However, we notice that the edge plasma is distinctly different in the two devices in two properties. First, the radial magnetic field in REPUTE edge is likely larger than in MST. REPUTE experiences resistive wall instabilities since its shell penetration time is short (1 ms versus > 100 ms in MST). REPUTE also has larger field errors arising from larger ports and toroidal field ripple. Second, the REPUTE edge [8] is collisional ($n \sim 2 \times 10^{19}$ m^{-3}, $T_e \sim 10$ eV) with an electron mean free path $\lambda_e \sim$ several cm, shorter than the parallel correlation length of the stochastic field $L_\parallel \sim 35$ cm, whereas the MST edge is relatively collisionless ($n \sim 2 \times 10^{18}$ m^{-3}, $T_e \sim 30$ eV) with $\lambda_e (\sim 2\text{ m}) > L_\parallel (\sim 1\text{ m})$.

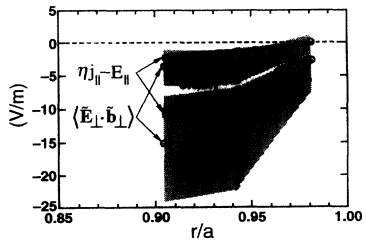

FIG. 5. Edge radial profiles of MHD dynamo electric field $\langle \tilde{E}_\perp \cdot \tilde{b}_\perp \rangle$ and $\eta j_\parallel - E_\parallel$ between and during the sawtooth crashes. The shaded region (blackened region) indicates the measurement uncertainty of $\langle \tilde{E}_\perp \cdot \tilde{b}_\perp \rangle$ ($\eta j_\parallel - E_\parallel$). Here the measurement uncertainty is determined from the ranges of rapid oscillations of Fig. 4.

In the KDT model [2], the strength of kinetic dynamo effect is gauged by the parameter $\lambda_e L_\parallel \tilde{b}_r^2/a^2$. Hence the possibly larger "static" $\tilde{b}_r$ in REPUTE would amplify the kinetic dynamo mechanism, relative to MST.

The effect of collisionality is more difficult to assess. The above KDT parameter would imply that the relatively collisionless MST is more prone to the kinetic dynamo. On the other hand, a collisionless model by Terry and Diamond [16] which incorporates self-consistency constraints (i.e., the effect of electron motion on the fluctuations through Ampere's law) predicts negligible current diffusion by a kinetic dynamo mechanism. This prediction is consistent with the large value of the measured MHD dynamo in MST. Moreover, the self-consistency constraint may not apply to the collisional REPUTE edge, particularly if the fluctuations are partly external (i.e., due to field errors).

Experimental indication of the possible presence of the kinetic dynamo first arose from observations in the ZT-40M RFP [5] of a small population of fast electrons (described by a half Maxwellian distribution). However, no direct measurements of the dynamo were performed. ZT-40M has similar radial field fluctuations to MST but its edge is more collisional ($n \sim 1 \times 10^{19}$ m^{-3}, $T_e \sim 20$ eV) with $\lambda_e L_\parallel \lesssim 0.5$. The fast electrons indeed carry most of $j_\parallel$ in the MST edge, but their properties [6] are different than those in ZT-40M. The MST population fits a drifted Maxwellian, is less energetic ($T_{e\parallel}^{\text{fast}}/T_e^{\text{bulk}} = 2-3$, $T_{e\perp}^{\text{fast}}/T_e^{\text{bulk}} \sim 1$), and is more dense ($n^{\text{fast}}/n^{\text{bulk}} \sim 20\%$). (Perhaps these differences suggest that the fast electrons in MST may be generated by a different mechanism, e.g., by the local MHD dynamo electric field.) Much higher T_e^{fast} ($\simeq 350$ eV) in ZT-40M than in MST results in larger KDT parameter for the fast electrons $\lambda_e^{\text{fast}} L_\parallel \tilde{b}_r^2/a^2$ ($\propto \lambda_e^{\text{fast}}/L_\parallel$ when $\tilde{b}_r^2$ is unchanged and $L_\parallel \propto a$), suggesting that ZT-40M may be more prone to the kinetic dynamo. Clearly, a comprehensive interpretation of the differences between these three experiments awaits the development of a collisional, self-consistent kinetic dynamo theory.

In conclusion, time-resolved measurements of discrete and continuous MHD dynamo have been performed in MST RFP edge. The observed MHD dynamo electric field is sufficient to sustain the parallel current. We speculate that observed different dynamo mechanisms in different machines depend upon the edge conditions, such as the presence of field errors or the collisionality. A comprehensive physical picture of the dynamo phenomena requires measurement of the MHD dynamo electric field under varying plasma conditions, and direct measurement of current diffusion (e.g., $\langle \tilde{P}_\parallel^e \tilde{b}_r \rangle$).

The authors are grateful to MST group members, particularly Dr. S. Hokin, Dr. I. H. Tan, Dr. W. Shen, and Dr. M. Stoneking, for their experimental contributions, and to Professor P. Terry and Professor Z. Yoshida for valuable discussions. This work was supported by the U.S. Department of Energy.

[1] C. G. Gimblett and M. L. Watkins, in *Proceedings of the 7th European Conference on Controlled Fusion and Plasma Physics, Lausanne, 1975* (European Physical Society, Geneva, 1975), Vol. 1, p. 103.
[2] A. R. Jacobson and R. W. Moses, Phys. Rev. A 29, 3335 (1984).
[3] R. W. Moses, K. F. Schoenberg, and D. A. Baker, Phys. Fluids, **31**, 3152 (1988).
[4] K. F. Schoenberg and R. W. Moses, Phys. Fluids B **3**, 1467 (1991).
[5] J. C. Ingraham *et al.*, Phys. Fluids B **2**, 143 (1990).
[6] M. R. Stoneking *et al.*, Bull. Am. Phys. Soc. **38**, 1978 (1993); (to be published).
[7] For example, the earliest simulation result is E. J. Caramana, R. A. Nebel, and D. D. Schnack, Phys. Fluids **26**, 1305 (1983); and the newest one is A. Nagata *et al.*, Phys. Fluids B **5**, 1263 (1993).
[8] H. Ji *et al.*, Phys. Rev. Lett. **69**, 616 (1992).
[9] A. al-Karkhy *et al.*, Phys. Rev. Lett. **70**, 1814 (1993).
[10] S. Hokin *et al.*, Phys. Fluids B **3**, 2241 (1991).
[11] L. Spitzer, Jr., *Physics of Fully Ionized Gases* (2nd Revised Edition) (Interscience Publishers, New York, 1962), p. 28.
[12] W. Shen and S. C. Prager, Phys. Fluids B **7**, 1931 (1993).
[13] R. N. Dexter *et al.*, Fusion Technol. **19**, 131 (1991).
[14] H. Ji *et al.*, Rev. Sci. Instrum. **62**, 2326 (1991). The inductive components are negligible in MST.
[15] A. F. Almagri *et al.*, Phys. Fluids B **4**, 4080 (1992).
[16] P. W. Terry and P. H. Diamond, Phys. Fluids B **2**, 1128 (1990).

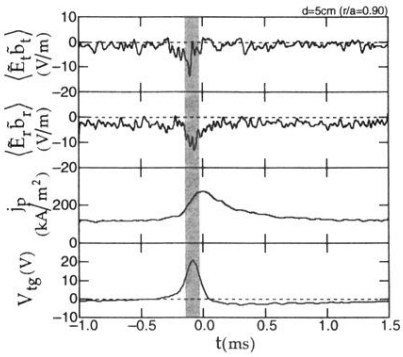

FIG. 3. Ensemble-averaged MHD dynamo electric fields and local parallel current density during one sawtooth crash, measured at $r/a = 0.90$.

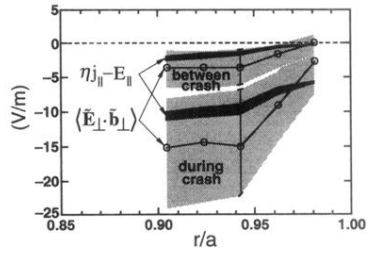

FIG. 5. Edge radial profiles of MHD dynamo electric field $\langle \tilde{\boldsymbol{E}}_{\perp} \cdot \tilde{\boldsymbol{b}}_{\perp} \rangle$ and $\eta j_{\parallel} - E_{\parallel}$ between and during the sawtooth crashes. The shaded region (blackened region) indicates the measurement uncertainty of $\langle \tilde{\boldsymbol{E}}_{\perp} \cdot \tilde{\boldsymbol{b}}_{\perp} \rangle$ $(\eta j_{\parallel} - E_{\parallel})$. Here the measurement uncertainty is determined from the ranges of rapid oscillations of Fig. 4.